

CP-violating top-Higgs coupling in SMEFT

Vernon Barger,^{1,*} Kaoru Hagiwara,^{2,†} and Ya-Juan Zheng^{3,‡}

¹*Department of Physics, University of Wisconsin, Madison, WI 53706 USA*

²*KEK Theory Center and Sokendai, Tsukuba, Ibaraki 305-0801, Japan*

³*Faculty of Education, Iwate University, Morioka, Iwate 020-8550, Japan*

Abstract

The total cross section of the process $\mu^- \mu^+ \rightarrow \nu_\mu \bar{\nu}_\mu t \bar{t} H$ has strong dependence on the CP phase ξ of the top Yukawa coupling, where the ratio of $\xi = \pi$ and $\xi = 0$ (SM) grows to 670 at $\sqrt{s} = 30$ TeV, 3400 at 100 TeV. We study the cause of the strong energy dependence and identify its origin as the $(E/m_W)^2$ growth of the weak boson fusion sub-amplitudes, $W_L^- W_L^+ \rightarrow t \bar{t} H$, with the two W 's are longitudinally polarized. We repeat the study in the SMEFT framework where EW gauge invariance is manifest and find that the highest energy cross section is reduced to a quarter of the complex top Yukawa model result, with the same energy power. By applying the Goldstone boson (GB) equivalence theorem, we identify the origin of this strong energy growth of the SMEFT amplitudes as associated with the dimension-6 $\pi^- \pi^+ t \bar{t} H$ vertex, where π^\pm denotes the GB of W^\pm . We obtain the unitarity bound on the coefficient of the SMEFT operator by studying all $2 \rightarrow 2$ and $2 \rightarrow 3$ cross sections in the $J = 0$ channel.

* barger@pheno.wisc.edu

† kaoru.hagiwara@kek.jp

‡ yjzheng@iwate-u.ac.jp

Possible CP violation in the largest coupling of the SM, the top Higgs Yukawa coupling, has received interest because of its potential role in producing the baryon asymmetry of the universe [1–3]. The coupling has been measured at the LHC in $t\bar{t}H$ production [4–7], and in single top plus Higgs production [6–8]. Most phenomenological studies of CP asymmetries in the above processes have been performed by adopting a complex Yukawa coupling, which can be parametrized as

$$\mathcal{L}_{t\bar{t}H} = -gH\bar{t}(\cos \xi + i\gamma_5 \sin \xi)t \quad (1)$$

with real positive g and $|\xi| \leq \pi$. The SM Yukawa coupling is recovered by setting $g = g_{\text{SM}} = m_t/v$ where $v = 246$ GeV is the SM Higgs VEV. The above parametrization, or its variants such as $g \cos \xi = g_{\text{SM}}\kappa_H$ (CP-even), $g \sin \xi = g_{\text{SM}}\kappa_A$ (CP-odd), have been adopted in studying CP violating asymmetries which change sign according to the sign of CP phase ξ , in $pp \rightarrow t\bar{t}H$ [9–12], $e^-e^+ \rightarrow t\bar{t}H$ [1, 13, 14], single top plus H production at the LHC [11, 12, 15, 16].

In this paper, we report our findings on the use of the above CP violating Yukawa coupling, at future high energy colliders, in particular at muon colliders [17, 18]. Shown in

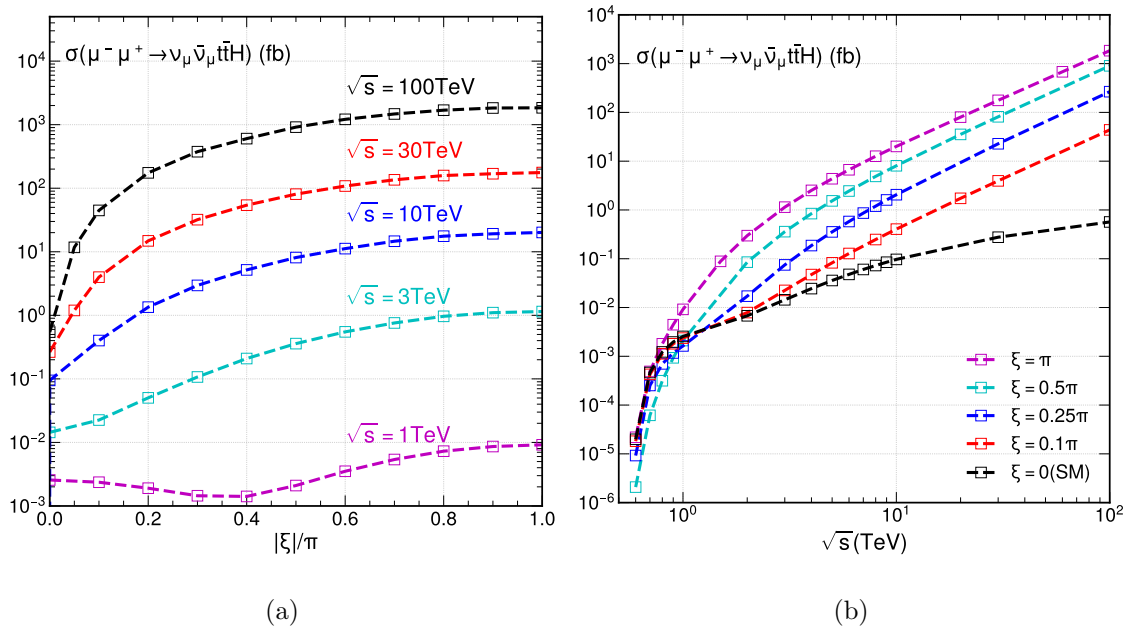


FIG. 1. Total cross section of $\nu_\mu \bar{\nu}_\mu t\bar{t}H$ production at a muon collider: (a) ξ dependence at several energies (b) \sqrt{s} dependence at several ξ values.

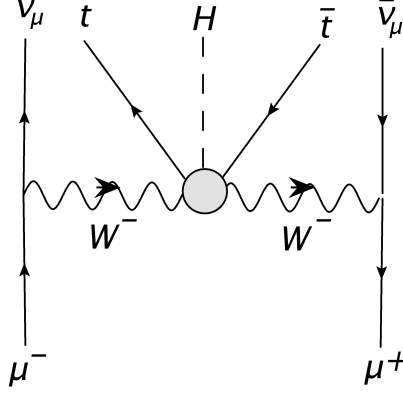


FIG. 2. Weak boson fusion subdiagrams, contributing to the process $\mu^- \mu^+ \rightarrow \nu_\mu \bar{\nu}_\mu t \bar{t} H$.

Fig. 1 is the total cross section of the process

$$\mu^- \mu^+ \rightarrow \nu_\mu \bar{\nu}_\mu t \bar{t} H \quad (2)$$

as a function of ξ for colliding muon energies in the range $0.6 \text{ TeV} \leq \sqrt{s} \leq 100 \text{ TeV}$. In the left hand side, Fig. 1(a), we show the cross section vs. $|\xi|/\pi$ at $\sqrt{s} = 1, 3, 10, 30, 100 \text{ TeV}$, whereas in the right hand side, Fig. 1(b), the \sqrt{s} dependence of the cross section is shown for $|\xi| = 0$ (SM), 0.1π , 0.25π , 0.5π and π .

In Fig. 1(a), we note a sharp rise of the cross section between $\xi = 0$ (SM) and $|\xi| \simeq 0.1\pi$ at very high energies ($\gtrsim 10 \text{ TeV}$), whereas in Fig. 1(b), we identify the quadratic energy behavior $(\sqrt{s})^2 = s$ of the total cross section above $\sqrt{s} \simeq 10 \text{ TeV}$, for all the non-zero ξ cases. In contrast, the SM cross section grows only logarithmically. We should understand the cause of this power behavior, and the importance on phenomenological studies on CP asymmetries in the process Eq. (2).

We study all the Feynman diagrams generated by `MadGraph5_aMC@NLO`[19], and identify that among 88 diagrams, 20 diagrams can be categorized as weak boson fusion (WBF) subprocesses, as depicted in Fig. 2. Since their contribution can be evaluated by making use of the weak boson PDF, we calculate the total cross section for the process

$$W^-(q, h = 0) W^+(\bar{q}, \bar{h} = 0) \rightarrow t \bar{t} H \quad (3)$$

where helicities $h = \bar{h} = 0$ represent longitudinal polarizations.

Shown in Fig. 3(a) is the total cross section as a function of \sqrt{s} , the colliding $W^- W^+$ or the $t \bar{t} H$ invariant mass, between 0.6 and 100 TeV. We can clearly identify the quadratic

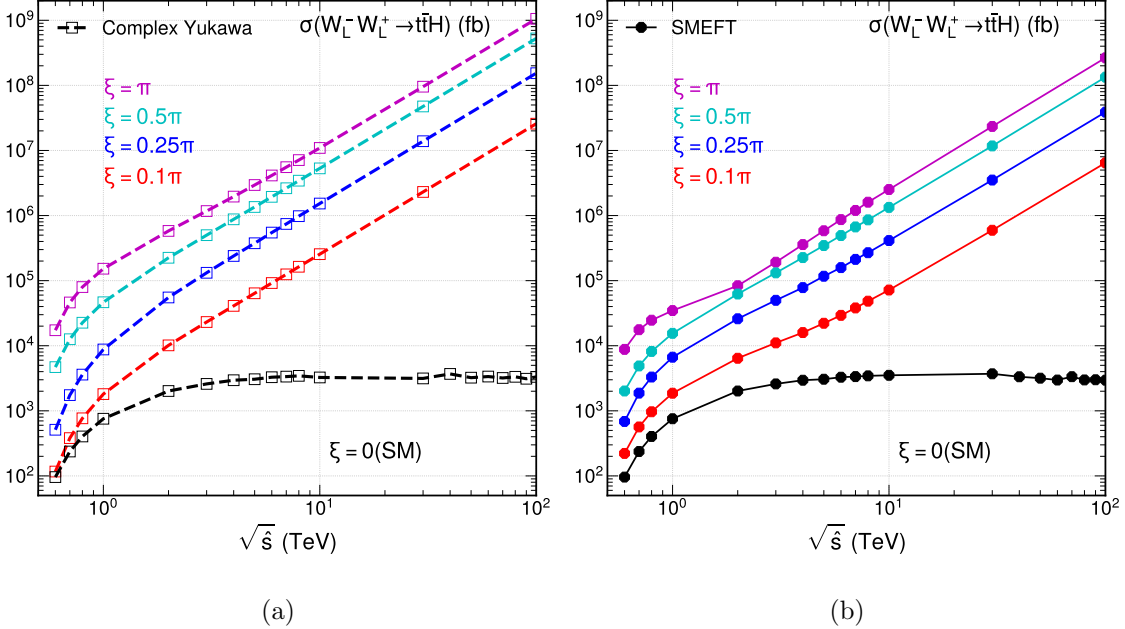


FIG. 3. $W_L^- W_L^+ \rightarrow t\bar{t}H$ cross section vs. the colliding $W^- W^+$ energy $\sqrt{\hat{s}}$: (a) complex Yukawa model and (b) SMEFT.

energy behavior of the total cross section for all non-zero ξ cases ($0.1\pi \leq |\xi| \leq \pi$) at energies above a few TeV. The quadratic energy power behavior of the total cross section is due to two powers of ξ of energy in the amplitudes from the incoming longitudinally polarized weak boson wave functions, which behave as E/m_W with $E = \sqrt{\hat{s}}/2$. In the SM, such powers of E/m_W are present in individual Feynman amplitudes, but they cancel after summing over all Feynman amplitudes, leading to the Goldstone boson equivalence theorem (GBET) as a manifestation of gauge invariance [20, 21].

We therefore look for gauge invariant formulation with a CP violating Yukawa coupling, such as arises from a two Higgs doublet model with a CP violating Higgs potential. When all the non-SM degrees of freedom are heavy, all such models can be reduced to SMEFT [22–25], and we identify the following top quark Yukawa sector[1, 26]¹

$$\mathcal{L} = -y_{\text{SM}} Q^\dagger \phi t_R + \frac{\lambda}{\Lambda^2} Q^\dagger \phi t_R \phi^\dagger \phi + \text{h.c.}, \quad (4)$$

with λ a complex number denoting the deviation from the SM. By inserting the component fields $Q = (t_L, b_L)^T$ and $\phi = ((v + H + i\pi^0)/\sqrt{2}, i\pi^-)^T$ into the Lagrangian Eq. (4), where

¹ The use of the SMEFT operator in Eq. (4) has been suggested by Cen Zhang to one of us in the year 2020, before he tragically passed away in 2021. The dimension-6 operator in eq.(4) is named $Q_{u\phi}$ in the Warsaw basis [24].

π^0 and π^\pm are the Goldstone bosons of Z and W^\pm , respectively, we find

$$\mathcal{L}_{ttH}^{\text{SMEFT}} = -Q^\dagger \phi t_R \left[y' - \frac{\lambda}{\Lambda^2} \left(vH + \frac{H^2 + (\pi^0)^2}{2} + \pi^+ \pi^- \right) \right] + \text{h.c.}, \quad (5)$$

where $y' = y_{\text{SM}} - \frac{\lambda v^2}{2\Lambda^2}$ is the Yukawa coupling including the SMEFT operator contribution². With $m_t = \frac{|y'|}{\sqrt{2}}v$, the phase $\arg(y')$ is absorbed by t_R and λ is re-phased accordingly. In the basis where we denote t_R and λ after the re-phasing, we can express the SMEFT Lagrangian Eq. (5) as

$$\begin{aligned} \mathcal{L}_{ttH}^{\text{SMEFT}} = & -m_t t_L^\dagger t_R - g_{\text{SM}} \left[(H + i\pi^0) t_L^\dagger + i\sqrt{2}\pi^- b_L^\dagger \right] t_R \\ & + (g_{\text{SM}} - ge^{i\xi}) \left\{ H t_L^\dagger t_R + \frac{H}{v} \left[(H + i\pi^0) t_L^\dagger + i\sqrt{2}\pi^- b_L^\dagger \right] t_R \right\} \\ & + (g_{\text{SM}} - ge^{i\xi}) \left\{ \left[\frac{H^2 + (\pi^0)^2}{2v} + \frac{\pi^+ \pi^-}{v} \right] t_L^\dagger t_R \right. \\ & \left. + \frac{H^2 + (\pi^0)^2 + 2\pi^+ \pi^-}{2v^2} \left[(H + i\pi^0) t_L^\dagger + i\sqrt{2}\pi^- b_L^\dagger \right] t_R \right\} + \text{h.c.}, \quad (6) \end{aligned}$$

where

$$g_{\text{SM}} = \frac{m_t}{v} \quad \text{and} \quad g_{\text{SM}} - ge^{i\xi} = \frac{\lambda v^2}{\sqrt{2}\Lambda^2}. \quad (7)$$

We maintain the original gauge invariant structure of the couplings in the above expression which agrees with ref.[27]. When we drop all terms proportional to Goldstone boson fields, it reduces to the results in ref.[26].

A few comments are in order. First, the ttH coupling of the SM, g_{SM} , is replaced by the complex coupling $ge^{i\xi}$, which is identical to the phenomenological Lagrangian Eq. (1). Second, although the ttH coupling is changed, the dimension-4 part of the Goldstone boson couplings remain the same as the SM. Third, the $ttHH$ coupling appears in the third and fourth terms, whereas the $ttHHH$ coupling appears in the last term. Fourth, all the vertices in the last term of the above Lagrangian have mass dimension-6, with 3 boson fields and a pair of fermion fields.

In the unitary gauge, only the $ttHH$ coupling

$$\mathcal{L}_{ttHH}^{\text{SMEFT}} = \frac{3(g_{\text{SM}} - ge^{i\xi})}{v} \frac{H^2}{2} t_L^\dagger t_R + \text{h.c.}, \quad (8)$$

² When the original Yukawa coupling y and the coefficient λ of the dimension-6 operator have the same flavor structure, we arrive at the flavor diagonal vertices as above. For a general treatment, see e.g. ref.[27].

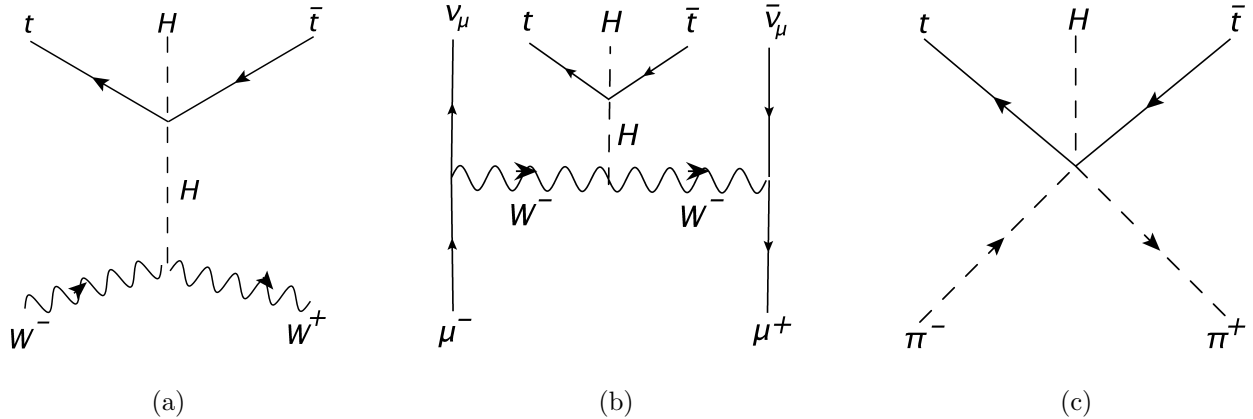


FIG. 4. Additional Feynman diagrams in SMEFT contributing to the process (a) $W_L^- W_L^+ \rightarrow t\bar{t}H$, (b) $\mu^- \mu^+ \rightarrow \nu_\mu \bar{\nu}_\mu t\bar{t}H$ in the unitary gauge, and (c) 5-point contact vertex $\pi^- \pi^+ t\bar{t}H$, giving the high energy limit of the $W_L^- W_L^+ \rightarrow t\bar{t}H$ amplitudes.

contributes to the weak boson fusion process Eq. (3) and to the muon collider process of Eq. (2). We modify the HELAS code[28, 29] of MadGraph5 to evaluate the amplitude of the Feynman diagram in Fig. 4(a) in the WW fusion process Eq. (3) and also the diagram Fig. 4(b) in the muon collider process Eq. (2).

By adding the diagram Fig. 4(a) to the 20 diagrams generated by MadGraph5 with the CP violating Yukawa coupling, we obtain the SMEFT amplitudes

$$\mathcal{M}(W_L^- W_L^+ \rightarrow t\bar{t}H)_{\text{SMEFT}} = \sum_{k=1}^{20} \mathcal{M}_k + \mathcal{M}_{\text{Fig. 4(a)}}, \quad (9)$$

which gives the total cross section in Fig.3(b) of the weak boson fusion process Eq. (3). We notice a significant reduction of the cross section at all energies, as compared to the results of the complex Yukawa coupling model which are shown in Fig.3(a). On the other hand, we find that the high energy power behavior of the total cross section is the same as that of the complex Yukawa model. Cross comparison of the two results, we find that when $\sqrt{\hat{s}} \gtrsim 10$ TeV

$$\sigma_{\text{tot}}(W_L^- W_L^+ \rightarrow t\bar{t}H)_{\text{SMEFT}} \approx \frac{1}{4} \sigma_{\text{tot}}(W_L^- W_L^+ \rightarrow t\bar{t}H)_{\text{complex Yukawa}} \quad (10)$$

for the same value of the complex Yukawa coupling, $ge^{i\xi}$.

In order to clarify our findings, we calculate the Goldstone boson scattering amplitudes for the process $\pi^- \pi^+ \rightarrow t\bar{t}H$ analytically, by using the SMEFT Lagrangian Eq. (6). At

high energies, the dimension-6 $\pi^-\pi^+t\bar{t}H$ vertex contribution dominates, as depicted by the diagram Fig. 4(c), and we find

$$\mathcal{M}_{\text{Fig. 4(c)}}^{\pm\pm} = \frac{1}{v^2} [\mp 2p_t (g_{\text{SM}} - g \cos \xi) - im_{t\bar{t}} (g \sin \xi)] \quad (11)$$

where p_t is the magnitude of t and \bar{t} momentum in the $t\bar{t}$ rest frame, $\pm\pm$ denotes t and \bar{t} helicities in the same frame, which should be common. Although the Higgs boson energy does not appear in the amplitude in Eq. (11), it is fixed as $E_H = \frac{\sqrt{\hat{s}}}{2} \left(1 + \frac{m_H^2 - m_{t\bar{t}}^2}{\hat{s}} \right)$, in the colliding W^-W^+ or $t\bar{t}H$ rest frame. Because the amplitude in Eq. (11) grows with the invariant mass of the $t\bar{t}$ pair, $m_{t\bar{t}}$, soft Higgs boson with energetic t and \bar{t} configuration dominates the total cross section at high energies. The total cross section

$$\sigma_{\text{tot}}(\pi^-\pi^+ \rightarrow t\bar{t}H) = \frac{1}{2\hat{s}} \sum_{h,\bar{h}=\pm 1/2} \int |\mathcal{M}^{h\bar{h}}|^2 d\Phi_{t\bar{t}H}, \quad (12)$$

obtained by using the above analytic amplitudes agree with the total cross section obtained by the numerical code in the unitary gauge at high energies. The linearly rising curves with the quadratic power of $\sqrt{\hat{s}}$ are reproduced by the Goldstone boson scattering cross section, verifying the GBET.

We therefore confirm that the SMEFT realization of the complex Yukawa coupling model[1, 26] reproduces all low energy phenomenology of the processes which are not affected by the $t\bar{t}HH$ coupling, and gives cross sections which are consistent with the GBET, as a consequence of the gauge invariance. However, the mystery remains. Why is the total cross section of the complex Yukawa model at high energies in Fig.3(a) four times the SMEFT cross section in Fig.3(b)?

In an attempt to clarify the above mystery, we compute analytically the only one additional diagram of the SMEFT in unitary gauge, Fig.4(a). We find that the only non-vanishing amplitudes are

$$\mathcal{M}_{\text{Fig. 4(a)}}^{\pm\pm} = \frac{3}{v^2} [\mp 2p_t (g_{\text{SM}} - g \cos \xi) - im_{t\bar{t}} (g \sin \xi)] \frac{(\hat{s} - 2m_W^2)}{(\hat{s} - m_H^2)}, \quad (13)$$

where the t and \bar{t} have the same helicities, $h = \bar{h} = \pm 1/2$, in the $t\bar{t}$ rest frame. Comparing the above amplitudes with the Goldstone boson amplitudes Eq. (11), we find

$$\mathcal{M}_{\text{Fig. 4(a)}}^{\pm\pm} = 3\mathcal{M}_{\text{Fig. 4(c)}}^{\pm\pm} \cdot \left\{ 1 + \mathcal{O}\left(\frac{1}{\hat{s}}\right) \right\}. \quad (14)$$

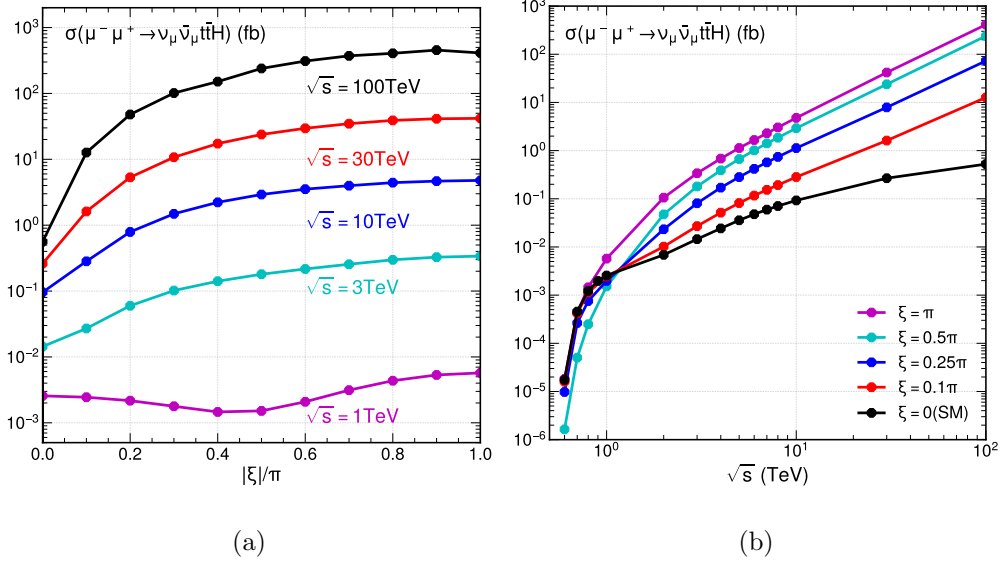


FIG. 5. Same as Fig.1 but for SMEFT.

On the other hand, the GBET for $\mathcal{M}(W_L^- W_L^+ \rightarrow t\bar{t}H)$ in Eq. (9) gives

$$\sum_{k=1}^{20} \mathcal{M}_k + \mathcal{M}_{\text{Fig. 4(a)}} = \mathcal{M}_{\text{Fig. 4(c)}} \cdot \left\{ 1 + \mathcal{O}\left(\frac{1}{\hat{s}}\right) \right\}. \quad (15)$$

Inserting Eq. (14), we find

$$\sum_{k=1}^{20} \mathcal{M}_k \approx -2\mathcal{M}_{\text{Fig. 4(c)}}, \quad (16)$$

at high energies. This explains why the sum of all the diagrams with CP violating Yukawa coupling gives 4 times the SMEFT cross section at high energies.

It suggests that there exists a Higgs sector, which reproduces the complex Yukawa coupling at dimension-4, but has no $ttHH$ coupling at dimension-5, and has the contact $\pi^-\pi^+ttH$ coupling at dimension-6 with minus two times that of the SMEFT Lagrangian Eq.(6). Within the framework of SMEFT, such Higgs sector is indeed found at dimension-8 level³. In this report, however, we proceed to study non-Standard Yukawa couplings in SMEFT at dimension-6 as in Eq.(6), which has no additional free parameters.

The total cross section of the muon collider process in Eq. (2) is now calculated in SMEFT by including the diagram Fig.4(b), which is evaluated numerically by using the HELAS code with the new vertex. The results are shown in Fig.5(a) for the ξ dependence at several col-

³ We thank Kun-Feng Lyu for suggesting us to examine dimension-8 operators.

lision energies, and in Fig.5(b) for the energy dependence at several $|\xi|$ values. When compared with the complex Yukawa model results of Fig.1(a) and (b), both the $|\xi|$ dependence and the energy dependence of the total cross section are milder in SMEFT. Nevertheless, the strong energy dependence of the total cross section remains, as a consequence of the $(\sqrt{\hat{s}})^2$ growth of the weak boson fusion cross section.

Before closing, we examine perturbative unitarity constraints of the SMEFT model of Eq. (4). The high energy amplitudes of the weak boson fusion process Eq. (3) is dominated by the $J = 0$ amplitudes, as is clear from the Goldstone boson amplitudes in Eq. (11) from the diagram Fig.4(c). We can therefore obtain constraints on the SMEFT operator from the scattering amplitudes of the $J = 0$ state of longitudinally polarized weak boson pair $|i\rangle = |W_L^- W_L^+(J=0)\rangle$. In the optical theorem

$$2\text{Im} \langle i|T|i\rangle = \sum_f |\langle f|T|i\rangle|^2, \quad (17)$$

tells that the final state $|f\rangle$ is summed over all $J = 0$ final states including the phase space integral. The unitarity bound $|\text{Im} \langle i|T|i\rangle| < |\langle i|T|i\rangle| < 16\pi$ can then be expressed as

$$\sum_f \sigma_{\text{tot}}(W_L^- W_L^+ \rightarrow f; J=0) < \frac{16\pi}{\hat{s}}. \quad (18)$$

All the SM cross sections fall as $1/\hat{s}$ at high energies in the $J = 0$ channel, and hence only

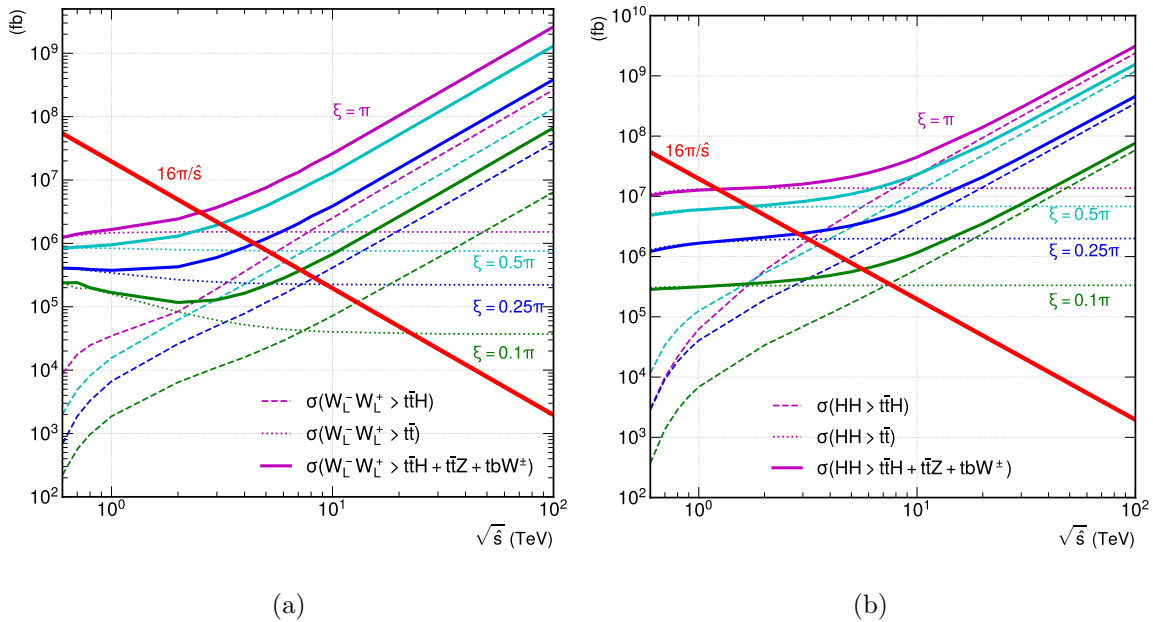


FIG. 6. Perturbative unitarity bound from $\sigma(W_L^- W_L^+ \rightarrow X)$ and $\sigma(HH \rightarrow X)$.

$ \xi $	π	0.5π	0.25π	0.1π
$ \lambda \cdot \Lambda^{-2}(\text{TeV}^{-2})$	32.9	23.2	12.6	5.14
$\sqrt{\hat{s}}_{W_L W_L}(\text{TeV})$	2.5	3.1	4.4	7.2
$\sqrt{\hat{s}}_{HH}(\text{TeV})$	1.2	1.7	2.9	5.6

TABLE I. Perturbative unitarity bounds from Fig. 6.

the contact SMEFT couplings are relevant. Examining the SMEFT Lagrangian of Eq. (6), we find that only one $2 \rightarrow 2$ process, $W_L^- W_L^+ \rightarrow t\bar{t}$ [26, 30, 31], and four $2 \rightarrow 3$ processes, $W_L^- W_L^+ \rightarrow t\bar{t}H, t\bar{t}Z, t\bar{b}W^-$ and $t\bar{b}W^+$, give non-vanishing total cross section at high energies.

In Fig. 6(a), we show the total cross section of the $t\bar{t}$ and $t\bar{t}H$ production processes in dotted and dashed lines respectively, and the sum of all the non-decreasing cross sections as a solid line as functions of colliding $W^- W^+$ energy, $\sqrt{\hat{s}}$, for several $|\xi|$ values. The unitarity bound of $16\pi/\hat{s}$ is shown by the straight solid line in red. The perturbative unitarity bound of the SMEFT model Eq. (4) can be read off from the crossing points for each $|\xi|$ value, which are tabulated in Table.I. Perturbative unitarity is violated at 2.5 TeV if $\xi = \pi$, or when $|\lambda|/\Lambda^2 = 32.9 \text{ TeV}^{-2}$, see Eq. (7).

From the Lagrangian Eq. (6) the $J = 0$ cross sections rise fastest in the HH channel, because of the large $ttHH$ and $ttHHH$ couplings. We show in Fig.6(b), the total cross sections of $HH \rightarrow t\bar{t}, t\bar{t}H$ and all final states in the $J = 0$ channel. The perturbative unitarity limit is significantly lower, 1.2 TeV for $|\xi| = \pi$, 5.6 TeV for $\xi = 0.1\pi$. Therefore, when viewing the SMEFT cross sections given in Fig.3(b), the curves can be trusted only below the energies in the bottom row of the table. In the muon collider process Eq. (2), we should restrict use of the perturbative amplitudes to the region where $m(t\bar{t}H)$ is below the bounds in the WW fusion subprocess.

We note that all the SMEFT cross sections presented in this paper have been obtained by treating the Lagrangian Eq. (6) as a gauge invariant version of the complex Yukawa coupling Eq. (1). When there are two ttH vertices in a Feynman diagram, both are replaced by the complex couplings, and thus the amplitude contains Λ^{-4} terms. The perturbative unitarity bounds in Table.I are valid since the $J = 0$ amplitudes at high energies are dominated by the dimension five and six vertices. Phenomenology of CP asymmetries in the EFT framework

are reported elsewhere [32].

ACKNOWLEDGEMENT

We are indebted to the late Cen Zhang for suggesting that we examine the SMEFT operator for the CP violating top Yukawa coupling. Throughout this study, we appreciated his deep insights on how we should look for non-Standard physics. It is a great loss for us that we cannot learn from him any more. We would like to thank Kenichi Hikasa, Kun-Feng Lyu and Kentarou Mawatari for very helpful discussions. YJZ thanks Ian Lewis and KC Kong for collaboration at early stage of this work. VB gratefully acknowledges support from the William F. Vilas Estate. KH is supported by the US Japan Cooperation Program in High Energy Physics. YJZ is supported by JSPS KAKENHI Grant No.21H01077 and 23K03403.

-
- [1] X. Zhang, S. K. Lee, K. Whisnant, and B. L. Young, “Phenomenology of a nonstandard top quark Yukawa coupling,” *Phys. Rev. D* **50** (1994) 7042–7047, [arXiv:hep-ph/9407259](#).
 - [2] E. Fuchs, M. Losada, Y. Nir, and Y. Viernik, “ CP violation from τ , t and b dimension-6 Yukawa couplings - interplay of baryogenesis, EDM and Higgs physics,” *JHEP* **05** (2020) 056, [arXiv:2003.00099](#) [[hep-ph](#)].
 - [3] H. Bahl, E. Fuchs, S. Heinemeyer, J. Katzy, M. Menen, K. Peters, M. Saimpert, and G. Weiglein, “Constraining the CP structure of Higgs-fermion couplings with a global LHC fit, the electron EDM and baryogenesis,” *Eur. Phys. J. C* **82** (2022) no. 7, 604, [arXiv:2202.11753](#) [[hep-ph](#)].
 - [4] **ATLAS** Collaboration, M. Aaboud *et al.*, “Observation of Higgs boson production in association with a top quark pair at the LHC with the ATLAS detector,” *Phys. Lett. B* **784** (2018) 173–191, [arXiv:1806.00425](#) [[hep-ex](#)].
 - [5] **CMS** Collaboration, A. M. Sirunyan *et al.*, “Measurements of $t\bar{t}H$ Production and the CP Structure of the Yukawa Interaction between the Higgs Boson and Top Quark in the Diphoton Decay Channel,” *Phys. Rev. Lett.* **125** (2020) no. 6, 061801, [arXiv:2003.10866](#) [[hep-ex](#)].

- [6] **ATLAS** Collaboration, G. Aad *et al.*, “ CP Properties of Higgs Boson Interactions with Top Quarks in the $t\bar{t}H$ and tH Processes Using $H \rightarrow \gamma\gamma$ with the ATLAS Detector,” *Phys. Rev. Lett.* **125** (2020) no. 6, 061802, [arXiv:2004.04545 \[hep-ex\]](#).
- [7] **ATLAS** Collaboration, “Probing the CP nature of the top-Higgs Yukawa coupling in $t\bar{t}H$ and tH events with $H \rightarrow b\bar{b}$ decays using the ATLAS detector at the LHC,” [arXiv:2303.05974 \[hep-ex\]](#).
- [8] **CMS** Collaboration, A. M. Sirunyan *et al.*, “Search for associated production of a Higgs boson and a single top quark in proton-proton collisions at $\sqrt{s} = 13$ TeV,” *Phys. Rev. D* **99** (2019) no. 9, 092005, [arXiv:1811.09696 \[hep-ex\]](#).
- [9] X.-G. He, G.-N. Li, and Y.-J. Zheng, “Probing Higgs boson CP Properties with $t\bar{t}H$ at the LHC and the 100 TeV pp collider,” *Int. J. Mod. Phys. A* **30** (2015) no. 25, 1550156, [arXiv:1501.00012 \[hep-ph\]](#).
- [10] H. Bahl, P. Bechtle, S. Heinemeyer, J. Katzy, T. Klingl, K. Peters, M. Saimpert, T. Stefaniak, and G. Weiglein, “Indirect CP probes of the Higgs-top-quark interaction: current LHC constraints and future opportunities,” *JHEP* **11** (2020) 127, [arXiv:2007.08542 \[hep-ph\]](#).
- [11] H. Bahl and S. Brass, “Constraining CP -violation in the Higgs-top-quark interaction using machine-learning-based inference,” *JHEP* **03** (2022) 017, [arXiv:2110.10177 \[hep-ph\]](#).
- [12] T. Martini, R.-Q. Pan, M. Schulze, and M. Xiao, “Probing the CP structure of the top quark Yukawa coupling: Loop sensitivity versus on-shell sensitivity,” *Phys. Rev. D* **104** (2021) no. 5, 055045, [arXiv:2104.04277 \[hep-ph\]](#).
- [13] K. Hagiwara, H. Yokoya, and Y.-J. Zheng, “Probing the CP properties of top Yukawa coupling at an e^+e^- collider,” *JHEP* **02** (2018) 180, [arXiv:1712.09953 \[hep-ph\]](#).
- [14] K. Cheung, Y.-n. Mao, S. Moretti, and R. Zhang, “Testing CP -violation in a Heavy Higgs Sector at CLIC,” [arXiv:2304.04390 \[hep-ph\]](#).
- [15] V. Barger, K. Hagiwara, and Y.-J. Zheng, “Probing the Higgs Yukawa coupling to the top quark at the LHC via single top+Higgs production,” *Phys. Rev. D* **99** (2019) no. 3, 031701, [arXiv:1807.00281 \[hep-ph\]](#).
- [16] V. Barger, K. Hagiwara, and Y.-J. Zheng, “Probing the top Yukawa coupling at the LHC via associated production of single top and Higgs,” *JHEP* **09** (2020) 101, [arXiv:1912.11795 \[hep-ph\]](#).

- [17] H. Al Ali *et al.*, “The muon Smasher’s guide,” *Rept. Prog. Phys.* **85** (2022) no. 8, 084201, [arXiv:2103.14043 \[hep-ph\]](#).
- [18] C. Aime *et al.*, “Muon Collider Physics Summary,” [arXiv:2203.07256 \[hep-ph\]](#).
- [19] J. Alwall, R. Frederix, S. Frixione, V. Hirschi, F. Maltoni, O. Mattelaer, H. S. Shao, T. Stelzer, P. Torrielli, and M. Zaro, “The automated computation of tree-level and next-to-leading order differential cross sections, and their matching to parton shower simulations,” *JHEP* **07** (2014) 079, [arXiv:1405.0301 \[hep-ph\]](#).
- [20] J. M. Cornwall, D. N. Levin, and G. Tiktopoulos, “Derivation of Gauge Invariance from High-Energy Unitarity Bounds on the S Matrix,” *Phys. Rev. D* **10** (1974) 1145. [Erratum: *Phys.Rev.D* **11**, 972 (1975)].
- [21] M. S. Chanowitz and M. K. Gaillard, “The TeV Physics of Strongly Interacting W’s and Z’s,” *Nucl. Phys. B* **261** (1985) 379–431.
- [22] C. N. Leung, S. T. Love, and S. Rao, “Low-Energy Manifestations of a New Interaction Scale: Operator Analysis,” *Z. Phys. C* **31** (1986) 433.
- [23] W. Buchmuller and D. Wyler, “Effective Lagrangian Analysis of New Interactions and Flavor Conservation,” *Nucl. Phys. B* **268** (1986) 621–653.
- [24] B. Grzadkowski, M. Iskrzynski, M. Misiak, and J. Rosiek, “Dimension-Six Terms in the Standard Model Lagrangian,” *JHEP* **10** (2010) 085, [arXiv:1008.4884 \[hep-ph\]](#).
- [25] F. Maltoni, L. Mantani, and K. Mimasu, “Top-quark electroweak interactions at high energy,” *JHEP* **10** (2019) 004, [arXiv:1904.05637 \[hep-ph\]](#).
- [26] K. Whisnant, B.-L. Young, and X. Zhang, “Unitarity and anomalous top quark Yukawa couplings,” *Phys. Rev. D* **52** (1995) 3115–3118, [arXiv:hep-ph/9410369](#).
- [27] J. Brod, J. M. Cornell, D. Skodras, and E. Stamou, “Global constraints on Yukawa operators in the standard model effective theory,” *JHEP* **08** (2022) 294, [arXiv:2203.03736 \[hep-ph\]](#).
- [28] K. Hagiwara, H. Murayama, and I. Watanabe, “Search for the Yukawa interaction in the process $e^+ e^- \rightarrow t \text{ anti-}t Z$ at TeV linear colliders,” *Nucl. Phys. B* **367** (1991) 257–286.
- [29] H. Murayama, I. Watanabe, and K. Hagiwara, “HELAS: HELicity amplitude subroutines for Feynman diagram evaluations,” *KEK-91-11* (1, 1992) .
- [30] M. Chen and D. Liu, “Top Yukawa Coupling at the Muon Collider,” [arXiv:2212.11067 \[hep-ph\]](#).

- [31] Z. Liu, K.-F. Lyu, I. Mahbub, and L.-T. Wang, “Top Yukawa Coupling Determination at High Energy Muon Collider,” [arXiv:2308.06323](#) [hep-ph].
- [32] V. Barger, K. Hagiwara, J. Kanzaki, K. Mawatari, and Y.-J. Zheng, “in preparation,”.